

Article

Substantially Enhanced Stereocomplex Crystallization of Poly(L-lactide)/Poly(D-lactide) Blends by the Formation of Multi-Arm Stereo-Block Copolymers

Xingyuan Diao, Xiaonan Chen, Shihao Deng and Hongwei Bai * 

College of Polymer Science and Engineering, State Key Laboratory of Polymer Materials Engineering, Sichuan University, Chengdu 610065, China; diaoxingyuan@stu.scu.edu.cn (X.D.); chenxiaonan@stu.scu.edu.cn (X.C.); dengshihao@stu.scu.edu.cn (S.D.)

* Correspondence: hongweibai@scu.edu.cn or bhw_168@163.com; Tel./Fax: +86-28-8546-0953

Abstract: Stereocomplex-type polylactide (SC-PLA) created by alternate packing of poly(L-lactide) (PLLA) and poly(D-lactide) (PDLA) chains in a crystalline state has emerged as a growingly popular engineering bioplastic that possesses excellent hydrolytic stability and thermomechanical properties. However, it is extremely difficult to acquire high-performance SC-PLA products via melt-processing of high-molecular-weight PLLA/PDLA blends because both SC crystallites and homocrystallites (HCs) are competitively formed in the melt-crystallization. Herein, a facile yet powerful way was employed to boost SC formation by introducing trace amounts of some epoxy-functionalized small-molecule modifiers into the enantiomeric blends during reactive melt-blending. The results show that the SC formation is considerably enhanced with the in situ generation of multi-arm stereo-block PLA copolymers, based on the reaction between epoxy groups of the modifiers and hydroxyl end groups of PLAs. More impressively, it is intriguing to find that the introduction of only 0.5 wt% modifiers can induce exclusive SC formation in the blends upon isothermal and non-isothermal melt-crystallizations. The outstanding SC crystallizability might be attributed to the suppressing effect of such unique copolymers on the separation of the alternately arranged PLLA/PDLA chain segments in molten state as a compatibilizer. Furthermore, the generation of these copolymers does not result in a significant increase in melt viscosity of the blends. These findings suggest new opportunities for the high-throughput processing of SC-PLA materials into useful products.

Keywords: polylactide; stereocomplex; crystallization; copolymer; compatibilization



Citation: Diao, X.; Chen, X.; Deng, S.; Bai, H. Substantially Enhanced Stereocomplex Crystallization of Poly(L-lactide)/Poly(D-lactide) Blends by the Formation of Multi-Arm Stereo-Block Copolymers. *Crystals* **2022**, *12*, 210. <https://doi.org/10.3390/cryst12020210>

Academic Editors: Jun Xu, Rufina G. Alamo and Günter Reiter

Received: 11 January 2022

Accepted: 27 January 2022

Published: 30 January 2022

Publisher's Note: MDPI stays neutral with regard to jurisdictional claims in published maps and institutional affiliations.



Copyright: © 2022 by the authors. Licensee MDPI, Basel, Switzerland. This article is an open access article distributed under the terms and conditions of the Creative Commons Attribution (CC BY) license (<https://creativecommons.org/licenses/by/4.0/>).

1. Introduction

In the past few decades, biodegradable polylactide (PLA) produced from bio-renewable feedstocks has aroused great repercussions because of its appealing physicochemical properties, such as favorable biocompatibility, excellent transparency, and high mechanical strength and stiffness [1–5]. To date, sustainable PLA has been increasingly utilized in biomedical materials and disposable commodities (e.g., food packaging and tableware). Nevertheless, its engineering applications have been greatly limited by the weak resistances to heat deformation and hydrolytic degradation [6–9]. Fortunately, it has been widely reported that stereocomplex (SC) crystallization between enantiomeric poly(L-lactide) (PLLA) and poly(D-lactide) (PDLA) chains can substantially increase the competitive edge of PLA over some petroleum-based engineering plastics (e.g., polycarbonate) [10–13]. Distinctly different from the common homocrystallization (HC), both L- and D-chains are compactly and alternately packed in the SC crystallization and, thereby, the SC-type PLA (SC-PLA) possesses superior heat resistance, hydrolytic stability, toughness, and gas barrier [11,14–16]. The melting temperature (T_m) of SC-PLA can be raised to nearly 230 °C, which is ca. 60 °C higher than that of PLA homopolymers with the same high crystallinity [6,17–19]. However, the SC crystallization is competitive with HC upon cooling from the melt of

PLLA/PDLA blends, especially when the molecular weight (MW) exceeds a critical value of 1×10^5 g/mol that is essential for attaining the necessary mechanical properties and melt-processability [20–24]. In general, homocrystallites (HCs) are predominantly formed over the SC crystallites during the melt-crystallization and processing of high-MW PLLA/PDLA blends, thus giving rise to the products having drastically decreased properties [21,25–28]. That is to say, the weak SC crystallizability makes it challenging to fabricate useful SC-PLA products using industrial melt-processing technologies. Accordingly, boosting SC crystallization of PLLA/PDLA blends is of vital importance for practical applications of the fascinating SC-PLA materials.

Until now, several strategies have been adopted to exploit PLLA/PDLA blends possessing exceptional SC crystallizability, such as block copolymerization [23,26,29,30] and the preparation of PLAs with special molecular architectures [31–36]. In comparison with linear PLLA/PDLA blends, star-shaped and comblike ones have been proven to exhibit markedly enhanced SC crystallizability, probably owing to the favored interactions between enantiomeric PLA branches and the increased segment mobility [34,37–41]. Nevertheless, such unique PLAs have not been industrially produced up to now, so considerable efforts have recently been devoted to gain exclusive SC crystallization of commercial linear high-MW PLLA/PDLA blends by incorporating certain processing additives (e.g., plasticizers [42–44], compatibilizers [22,45,46], and nucleating agents [47–50]). For example, Yang et al. [51] first reported that poly (ethylene glycol) (PEG) can facilitate the SC crystallization of PLLA/PDLA blends by increasing segment mobility and diffusion ability as a plasticizer. The sole formation of SC crystallites can be obtained in the melt-crystallization of the blends with 10 wt% PEG having MW of 1000 or 2000 g/mol. Additionally, various miscible polymers (e.g., poly (methyl methacrylate) (PMMA) [52–54], poly(vinyl phenol) (PVPh) [55], and poly(vinyl acetate) (PVAc) [56]) have been successfully utilized as compatibilizers to enhance the SC crystallizability and simultaneously suppress the homo-crystallizability by increasing the intermolecular interactions between L- and D-chains. Unfortunately, their compatibilization efficiency for PLLA/PDLA blends seems to be very low, hence at least 30–75 wt% compatibilizers are required for the exclusive SC formation. In this case, the physicochemical properties and sustainable attributes of the SC-PLA could be significantly deteriorated. Very recently, we demonstrated that the introduction of trace amounts (e.g., 0.3–0.5 wt%) of epoxy-functionalized oligo(styrene-acrylic) (ESA) into the blends leads to the in situ generation of comb-like PLA-*graft*-ESA copolymers containing long PLLA/PDLA branches in the reactive melt-blending process, and these copolymers can behave as highly efficient compatibilizers to stimulate exclusive SC formation [57]. This indicates that reactive blending is a relatively facile and low-cost strategy to remarkably enhance the SC crystallizability of the high-MW enantiomeric blends without sacrificing their valuable properties. However, the generation of such comb-like copolymers with densely grafted long PLA branches also causes a remarkable rise in melt viscosity of the blends due to the greatly increased chain entanglement density [38,58]. This is beneficial to the melt-processing requiring high viscosity and melt strength (e.g., film molding, blow molding, and foaming), but extremely detrimental to that demanding relatively high melt flowability (e.g., thin-wall injection molding). Therefore, any strategy that could substantially enhance the SC crystallizability of PLLA/PDLA blends without evidently increasing their melt viscosity is highly desirable for the high-throughput fabrication of SC-PLA products using some melt-processing technologies like injection molding.

With this aim in mind, in this contribution, we attempt to construct multi-arm stereo-block copolymers in high-MW PLLA/PDLA (50/50) blends by introducing trace amounts of some small-molecule modifiers bearing fewer than five epoxy groups during melt-blending. It was anticipated that unique stereo-block PLA copolymers having 2–4 arms could be in situ generated in the reactive blending, based on the reaction between epoxy groups of the modifiers and hydroxyl end groups of enantiomeric PLLA/PDLA chains (as illustrated in Figure 1). As compared with the comb-like copolymers, the multi-arm PLA copolymers formed in the blends could have much less influence on the melt viscosity,

because the number of PLA chains in each copolymer molecule is significantly decreased. Beyond that, the SC crystallizability was also expected to be substantially enhanced as the multi-arm copolymers could also function as compatibilizers to suppress the separation of alternately arranged PLLA/PDLA chain segments (i.e., the ordered PLLA/PDLA chain assemblies) after complete melting (as illustrated in Figure 2). The isothermal and non-isothermal crystallization behaviors of the obtained blends were investigated, highlighting the critical role of the arm number of multi-arm PLA copolymers in boosting SC crystallizability for the first time. Our work could pave a straightforward way towards PLLA/PDLA blends with outstanding SC crystallizability and melt flowability, pushing forward the melt-processing and engineering applications of SC-PLA materials.

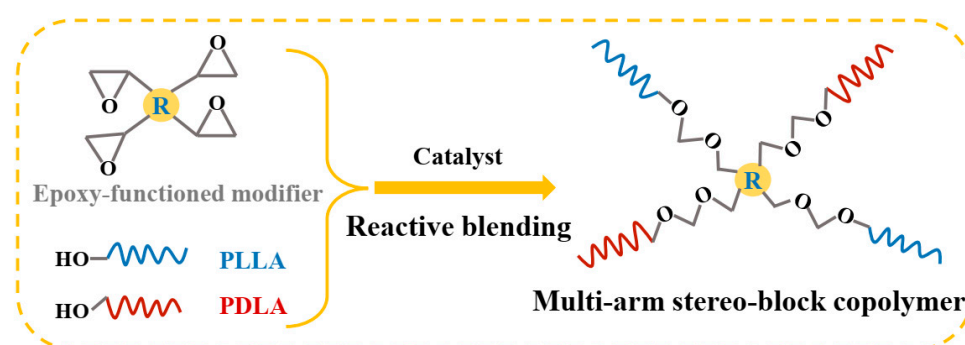


Figure 1. Schematic illustration of the reaction between epoxy-functionalized small-molecule modifiers and PLA chains for the in situ generation of multi-arm stereo-block PLA copolymers during melt-blending. Please note that the structure consisting of an equal number of PLLA and PDLA arms is only the ideal situation for such copolymers. The copolymers having unequal numbers of PLLA and PDLA arms could also be generated.

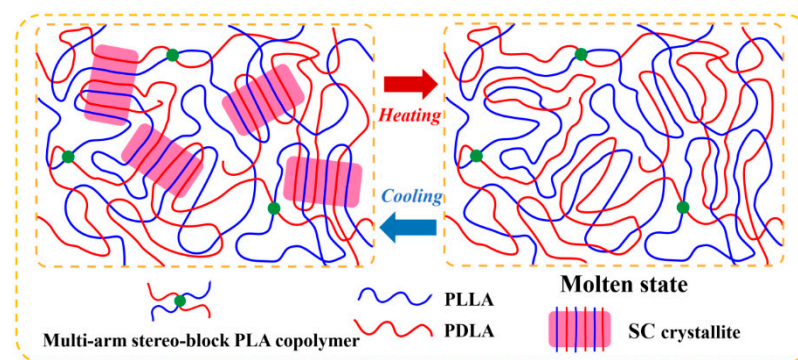


Figure 2. Schematic illustrating the plausible molecular mechanism for the enhanced SC crystallizability of PLLA/PDLA blends with multi-arm stereo-block PLA copolymers.

2. Materials and Methods

2.1. Materials

PLLA (D-isomer content = 1.5%, trade name 4032D) with a weight molecular weight (M_w) of 1.7×10^5 g/mol and a polydispersity index (PDI) of 1.7 was purchased from Nature Works LLC, USA. PDLA (L-isomer content = 1%, $M_w = 1.6 \times 10^5$ g/mol, PDI = 1.6) was obtained from Zhejiang Hisun Biomaterial Co. Ltd., Taizhou, China. Neopentyl glycol diglycidyl ether containing two epoxy groups (named as 2EG) was provided by Shanghai Aladdin Biochemical Technology Co. Ltd., Shanghai, China. Trimethylolpropane triglycidyl ether containing three epoxy groups (named as 3EG) and pentaerythritol glycidyl ether having four epoxy groups (named as 4EG) were purchased from Sigma-Aldrich (Shanghai) Trading Co. Ltd. and Shanghai Macklin Biochemical Co. Ltd., respectively. Triethylamine used as the catalyst was obtained from Shanghai Aladdin Biochemical Technology Co. Ltd.,

Shanghai, China. The 2EG, 3EG, and 4EG were utilized as the reactive modifiers (named as RMs), and their chemical structures are presented in Figure 3. All of the materials are commercially available. Both PLLA and PDLA pellets were pre-dried in a vacuum oven at 60 °C to avoid moisture-induced thermal degradation during subsequent melt-processing.

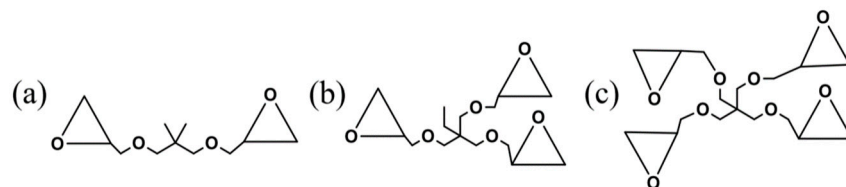


Figure 3. Chemical structures of the reactive modifiers: (a) neopentyl glycol diglycidyl ether (2EG), (b) trimethylolpropane triglycidyl ether (3EG), and (c) pentaerythritol glycidyl ether (4EG).

2.2. Sample Preparation

PLLA/PDLA (50/50) blends with different RMs were prepared by melt-blending using a Haake Rheomix 600 internal mixer (Karlsruhe, Germany) at a temperature of 200 °C, in the presence of 0.3 wt% triethylamine as a catalyst for the reaction between RMs and PLAs. The rotation speed and blending time were set as 60 rpm and 5 min, respectively. Prior to the melt-blending, the RMs and catalyst were pre-mixed in absolute ethanol to ensure their homogeneous dispersion in the blends. To simplify, the achieved PLLA/PDLA/RM blends were denoted as LD-*x*EG-*y*, in which *x* and *y* indicate the number of epoxy groups for each RM (*x* = 2, 3, 4) and the weight percentage of RMs.

2.3. Characterization and Measurements

2.3.1. Fourier Transform Infrared Spectroscopy (FT-IR)

Nicolet 6700 spectrometer (Thermo Fisher Scientific, Waltham, MA, USA) was used to characterize the generation of multi-arm PLA copolymers in the blends. The FT-IR spectra were recorded from 4000 to 400 cm⁻¹ at a resolution of 4 cm⁻¹ for 32 scans.

2.3.2. Rheological Testing

Rheological behaviors were measured using a Discovery HR-1 rheometer (TA Instruments, New Castle, DE, USA) equipped with two parallel plates (25 mm in diameter). The measurements were performed at 240 °C in the frequency sweep mode (0.01–100 Hz), under the protection of a dry nitrogen atmosphere. The strain used (1%) was within the linear viscoelastic region.

2.3.3. Differential Scanning Calorimetry (DSC)

Crystallization and melting behaviors were examined using a DSC 8000 (PerkinElmer, Waltham, MA, USA) under nitrogen atmosphere to avoid the thermal degradation of PLA chains. Samples of ca. 5–6 mg were sealed in an aluminum crucible before the examination. For the non-isothermal crystallization, the samples were completely melted at 250 °C for 3 min to erase the thermal history and then cooled to 30 °C at a scanning rate of 10 °C/min. In the isothermal crystallization, the samples were quenched (at a cooling rate of 150 °C/min) from 250 °C to a pre-set temperature (160 °C) and then kept at this temperature until the crystallization was completed. After the non-isothermal and isothermal crystallizations, the samples were re-heated to 250 °C at a rate of 10 °C/min to examine the melting behaviors. Based on the melting enthalpies of HC ($\Delta H_{m,HC}$) and SC crystallites ($\Delta H_{m,SC}$) obtained from the DSC heating curves, the crystallinity values of these crystallites were calculated using the following formulas:

$$X_{c,HC} = \frac{\Delta H_{m,HC}}{\Delta H_{m,HC}^0} \quad (1)$$

$$X_{c,SC} = \frac{\Delta H_{m,SC}}{\Delta H_{m,SC}^{\theta}} \quad (2)$$

$$X_c = X_{c,HC} + X_{c,SC} \quad (3)$$

where $X_{c,HC}$ and $X_{c,SC}$ represent the melting enthalpies of infinitely large HCs (93 J/g^{11}) and SC crystallites (142 J/g^{11}), respectively; while $X_{c,HC}$ and $X_{c,SC}$ are the crystallinity values of homocrystallites and SC crystallites, respectively; and X_c is the total crystallinity of the crystallites formed in the PLLA/PDLA blends.

The fraction of SC crystallites in the crystalline phase was estimated by the following expressions:

$$f_{sc} = \frac{X_{c,SC}}{X_{c,SC} + X_{c,HC}} \times 100\% \quad (4)$$

2.3.4. Wide-Angle X-ray Diffraction (WAXD)

WAXD patterns were collected using an X'Pert Pro MPD X-ray diffractometer (PANalytical, Holland) at room temperature. The diffractometer was equipped with a $\text{CuK}\alpha$ radiation ($\lambda = 0.154 \text{ nm}$) working at 40 kV and 40 mA. The scanning diffraction angle (2θ) ranged from 5° to 40° .

3. Results and Discussion

3.1. Generation of Multi-Arm Stereo-Block PLA Copolymers in PLLA/PDLA Blends

The PLLA/PDLA blends without and with epoxy-functionalized modifiers (RMs) were prepared by reactive melt-blending under the catalysis of 0.3 wt% triethylamine at 200°C , where multi-arm stereo-block PLA copolymers could be in situ generated (as illustrated in Figure 1) along with the stereocomplexation of enantiomeric PLA chains [38,57]. The coupling reaction between epoxy groups of the RMs and hydroxyl end groups of the PLAs was verified by FT-IR. Figure 4 gives the full and enlarged FT-IR spectra of PLLA/PDLA blends with various amounts of RM having four epoxy groups (i.e., 4EG). For assigning the characteristic bands, the FT-IR spectra of pure PLLA/PDLA blend and 4EG were also measured. Expectedly, the characteristic absorption peak at 908 cm^{-1} , belonging to the epoxy groups in 4EG, disappears after reactive blending. This means that most epoxy groups of RMs could be completely reacted with the end groups of PLAs to generate multi-arm stereo-block PLA copolymers in the blending.

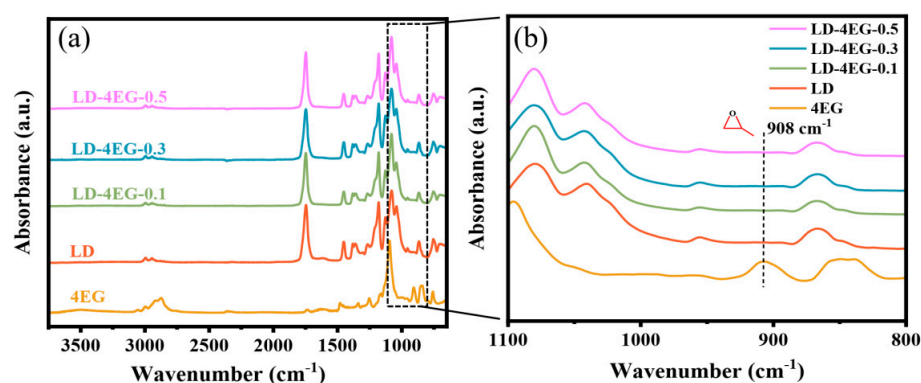


Figure 4. (a) Full and (b) enlarged FT-IR spectra of melt-quenched PLLA/PDLA blends with different loadings of 4EG.

The generation of such multi-arm PLA copolymers can be further confirmed by rheological testing, as shown in Figure 5. The storage modulus in the low-frequency region is highly sensitive to the presence of long-chain-branched and/or multi-arm structures in polymer melts owing to the increased interchain entanglement density [33,59]. It can be clearly seen from Figure 5a that adding a small amount of 4EG leads to an evident increase in the storage modulus of PLLA/PDLA blend at low frequencies (0.01–1 Hz). Moreover,

the discrepancy becomes more obvious with the increasing 4EG content up to 0.5 wt%. These results suggest that the multi-arm PLA copolymers have been successfully generated in the PLLA/PDLA/RM blends.

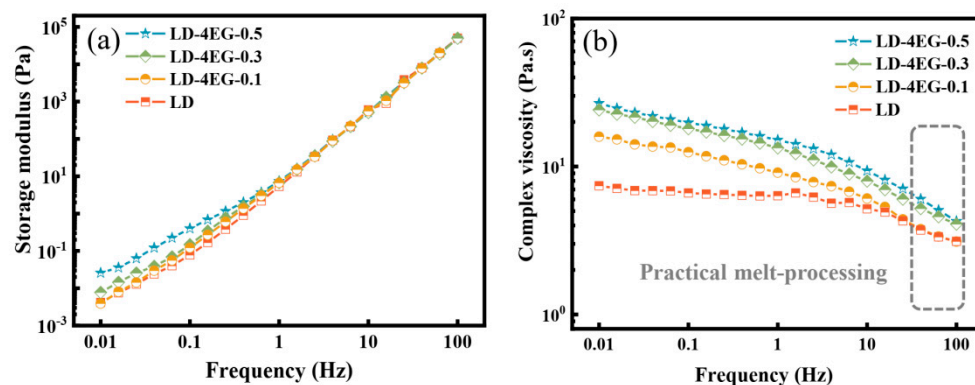


Figure 5. Rheological properties of PLLA/PDLA blends with different loadings of 4EG: (a) storage modulus and (b) complex viscosity as a function of angular frequency.

Furthermore, it is noteworthy that the melt viscosity of PLLA/PDLA blends in the shear rate range of 50–100 Hz (close to that in practical melt-processing including extrusion and injection molding, as highlighted in Figure 5b) is not pronouncedly increased with the generation of the multi-arm PLA copolymers, which is distinctly different from that observed in the blends with long-chain-branched PLA copolymers [8,60]. For example, the melt viscosity of PLLA/PDLA (50/50) blend at 100 Hz is only slightly enhanced from 3.1 Pa·s to 4.2 Pa·s with the addition of 0.5 wt% 4EG. This is highly favorable for the high-throughput processing of PLLA/PDLA blends in the industry.

3.2. Non-Isothermal Crystallization of PLLA/PDLA Blends

To explore the role of the multi-arm stereo-block PLA copolymers generated in enhancing the SC crystallizability of PLLA/PDLA blends, the non-isothermal melt-crystallization behaviors of the racemic blends without and with various amounts of 4EG were systematically analyzed using DSC and WAXD. Figure 6a,b exhibit their DSC cooling and the second heating curves, respectively. The crystallinity values of HCs ($X_{c,HC}$) and SC crystallites ($X_{c,SC}$) calculated from the DSC heating curves are plotted as a function of 4EG content and shown in Figure 6c. As expected, the generation of multi-arm PLA copolymers has a significant effect on the non-isothermal crystallization of the blends (Figure 6a). For the PLLA/PDLA blend without any RMs, the SC crystallization and HC are found to successively occur at ca. 126 °C and 110 °C, respectively, upon cooling from the blend melts. The formation of both HC and SC crystallites in the melt-crystallization process can be checked by the appearance of two characteristic melting peaks in the second heating curve at ca. 172 °C and 218 °C (Figure 6b), assigned to the melting of HC and SC crystallites, respectively. However, with the generation of multi-arm PLA copolymers in PLLA/PDL/4EG blends, the melting peak of SC crystallites enlarges evidently, while that of HC reduces remarkably, indicating that the SC crystallizability is greatly enhanced and the homo-crystallizability is notably suppressed at the same time (Figure 6a–c). With regard to the decrease in the crystallization temperature ($T_{c,SC}$) with the increasing 4EG content, it could be attributed to the disturbance effect of the multi-arm structures on the crystallization [59]. More impressively, the SC crystallites can be exclusively formed with further increasing 4EG content up to 0.5 wt%. These results vividly demonstrate that the generation of sufficient amounts of multi-arm PLA copolymers can substantially promote the SC crystallization of racemic PLLA/PDLA blends.

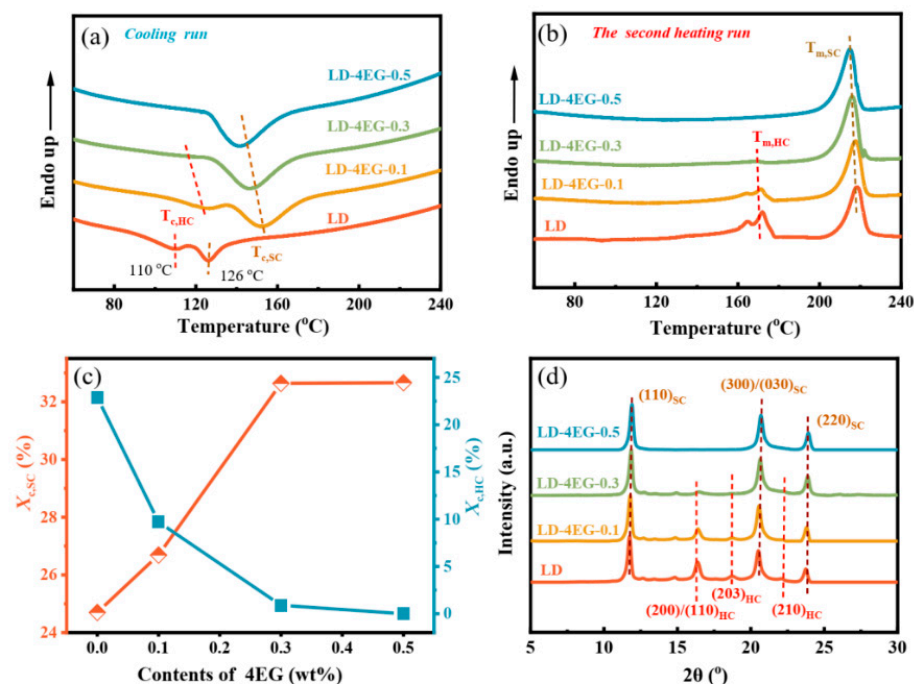


Figure 6. DSC thermograms of PLLA/PDLA/4EG blends collected during (a) cooling scans and (b) subsequent heating scans (the scanning rate was fixed at 10 °C/min); (c) crystallinity of HC and SC crystallites formed in the non-isothermal melt-crystallization as a function of 4EG content; and (d) WAXD patterns of the melt-crystallized blends.

WAXD patterns provide further evidence for the multi-arm PLA copolymers' induced enhancement in the SC crystallizability, as shown in Figure 6d. Expectedly, besides the characteristic diffraction peaks of SC crystallites appearing at around 12.1°, 21.0°, and 24.1°, the strong diffraction peaks of HCs can be observed in the WAXD pattern of the PLLA/PDLA blend without 4EG at 16.8°, 18.9°, and 22.4° [61], respectively. Nevertheless, in the case of PLLA/PDLA/4EG blends, the characteristic peaks of SC crystallites become stronger with the increasing 4EG content. Meanwhile, the diffractions of HC decrease markedly and diminish completely when the 4EG content reaches 0.5 wt%, indicating that the multi-arm stereo-block PLA copolymers generated in the blends have a strong ability to stimulate exclusive SC formation during the non-isothermal crystallization process.

3.3. Isothermal Crystallization of PLLA/PDLA Blends

To reveal the mechanism for the enhanced SC crystallizability of PLLA/PDLA blends with the generation of stereo-block PLA copolymers with unique multi-arm structures, the isothermal crystallization behaviors of the racemic blends without and with 0.5 wt% 4EG were studied at a high temperature of 160 °C, suitable for SC formation [18,62]. Figure 7 presents their DSC curves collected during isothermal crystallization and subsequent heating runs. Clearly, the PLLA/PDLA(50/50) blend exhibits not only a relatively slow crystallization process (the peak-time (t_p) is as high as 5.1 min, Figure 7a), but also the simultaneous formation of both HC and SC crystallites in the crystallization (Figure 7b), which is an indicator of the inferior SC crystallizability. Fascinatingly, with the addition of 0.5 wt% 4EG into the blend, t_p is significantly decreased to 2.3 min and the exclusive SC crystallization is triggered. This proves that the unique PLA copolymers enable the PLLA/PDLA blends to exclusively crystallize into SC crystallites at an accelerated crystallization rate.

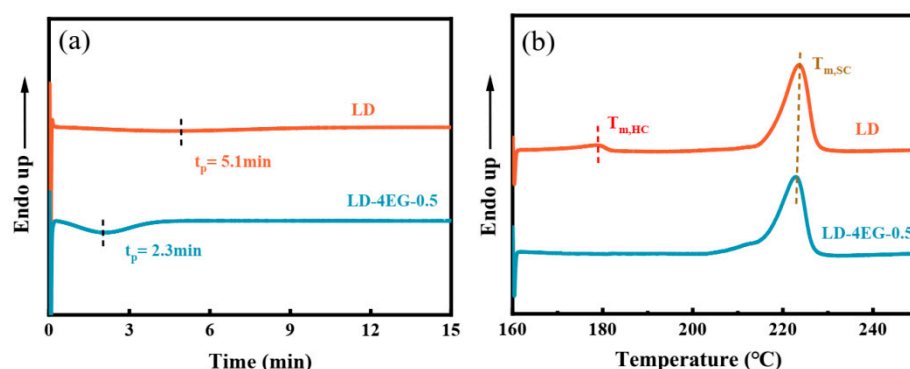


Figure 7. DSC thermograms of PLLA/PDLA blends without and with 0.5 wt% 4EG during (a) isothermal crystallization at 160 °C and (b) subsequent heating scans.

It has been well established that the survival of alternately arranged PLLA/PDLA chain segments in PLLA/PDLA blend melts plays a key role in their SC crystallization process because they can serve as a nucleation precursor to accelerate crystallization and stimulate exclusive SC formation [28,63]. In general, complete melting of high-MW PLLA/PDLA blends could lead to the separation of enantiomeric PLA chains into PLLA- and PDLA-rich domains, thus the SC formation in the phase-separated melts is kinetically limited by the prolonged chain diffusion pathway as compared with the formation of HCs [21,64]. However, the multi-arm stereo-block PLA copolymers could behave as compatibilizers to effectively suppress the separation of the ordered PLLA/PDLA segment assemblies, probably because their long PLA arms can readily interact with the PLLA and PDLA segments. Therefore, the generation of such PLA copolymers can impart the PLLA/PDLA blends with substantially enhanced SC crystallizability.

3.4. Crucial Role of the Arm Number of Multi-Arm Stereo-Block PLA Copolymers in Enhancing SC Crystallizability of PLLA/PDLA Blends

Considering that the arm number of multi-arm stereo-block PLA copolymers generated in PLLA/PDLA blends could play an important role in facilitating the SC crystallization, the crystallization behaviors of the racemic blends with different RMs were comparatively investigated. Figure 8 shows the DSC heating curves of these blends after non-isothermal melt-crystallization. It is interesting to find that the formation of SC crystallites in the melt-crystallized blends is markedly enhanced with the increasing number of epoxy groups in each RM (Figure 8a–c). As compared with PLLA/PDLA/2EG and PLLA/PDLA/3EG blends, more SC crystallites are formed in the crystallization of PLLA/PDLA/4EG blends with the same RM content (Figure 8d). More interestingly, the introduction of RMs with relatively high epoxy equivalent weights leads to the multi-arm PLA copolymers having a stronger ability to promote SC formation and, finally, exclusive SC formation can be obtained when the content of 4EG is higher than 0.3 wt%. These results suggest that increasing the arm number of the multi-arm PLA copolymers is favorable for the SC crystallization of PLLA/PDLA racemic blends by improving the suppressing effect on the separation of the ordered PLLA/PDLA segment assemblies in molten state.

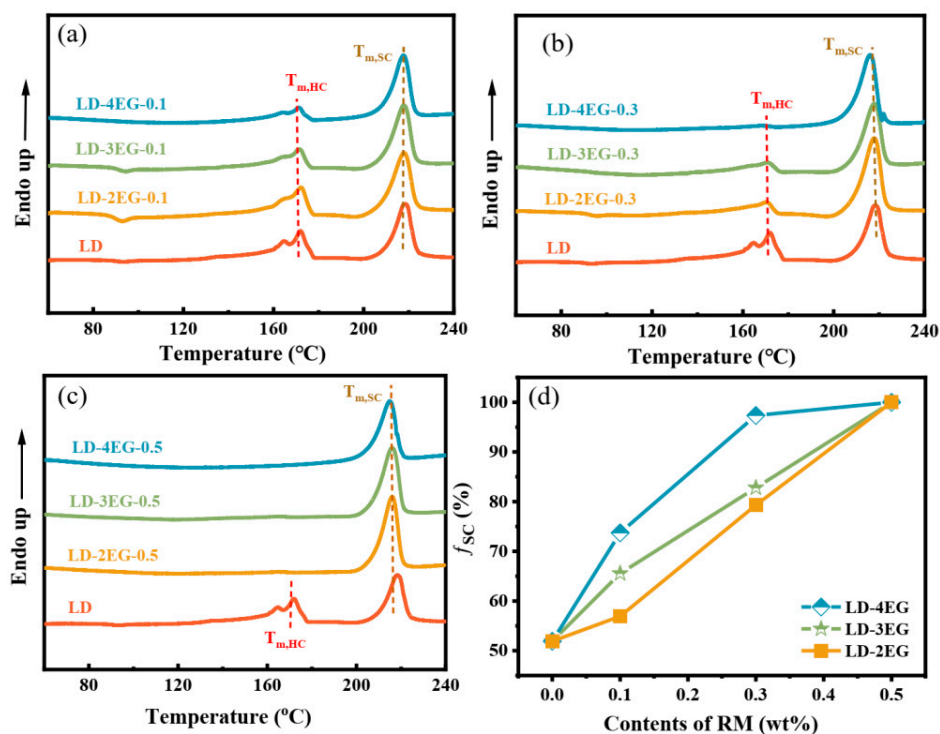


Figure 8. DSC heating curves of PLLA/PDLA blends with different loadings of RMs after cooling from the molten state at a rate of 10 °C/min: (a) 0.1 wt%, (b) 0.3 wt%, and (c) 0.5 wt%; (d) the fraction of SC crystallites (f_{sc}) formed in the non-isothermal melt-crystallization as a function of RM loading.

4. Conclusions

To summarize, small-molecule modifiers bearing several epoxy groups were successfully used to markedly enhance the SC crystallizability of PLLA/PDLA blends through in situ generation of multi-arm stereo-block PLA copolymers in reactive melt-blending. With the generation of such PLA copolymers with unique structures, the formation of SC crystallites is remarkably enhanced under both non-isothermal and isothermal melt-crystallization conditions. Notably, the exclusive SC formation can be achieved in the melt-crystallized blends containing only 0.5 wt% modifiers, suggesting a strong stabilizing effect of the copolymers on the alternately arranged PLLA/PDLA chain segments in molten state as effective compatibilizers. Moreover, the copolymers having relatively more arms are found to exhibit superior compatibilizing efficiency, as evidenced by the enhanced SC formation at lower modifier loadings. Most impressively, the generation of these copolymers does not greatly increase the melt viscosity of the racemic blends, which makes it possible to rapidly transform the blends into high-performance SC-PLA products via industrial melt-processing.

Author Contributions: Conceptualization, X.D. and X.C.; methodology, X.D.; software, X.D.; validation, X.D., X.C., and S.D.; formal analysis, S.D.; investigation, X.C.; resources, H.B.; data curation, X.C.; writing—original draft preparation, X.D.; writing—review and editing, H.B.; visualization, S.D.; supervision, H.B.; project administration, H.B.; funding acquisition, H.B. All authors have read and agreed to the published version of the manuscript.

Funding: National Natural Science Foundation of China (No. 51873129).

Data Availability Statement: Not applicable.

Acknowledgments: This work was financially supported by the National Natural Science Foundation of China (No. 51873129).

Conflicts of Interest: The authors declare no conflict of interest.

References

1. Nampoothiri, K.M.; Nair, N.R.; John, R.P. An overview of the recent developments in polylactide (PLA) research. *Bioresour. Technol.* **2010**, *101*, 8493–8501. [[CrossRef](#)] [[PubMed](#)]
2. Liu, G.; Zhang, X.; Wang, D. Tailoring crystallization: Towards high-performance poly(lactic acid). *Adv. Mater.* **2014**, *26*, 6905–6911. [[CrossRef](#)] [[PubMed](#)]
3. Huang, S.M.; Hwang, J.J.; Liu, H.J.; Zheng, A.M. A characteristic study of polylactic acid/organic modified montmorillonite (PLA/OMMT) nanocomposite materials after hydrolyzing. *Crystals* **2021**, *11*, 376. [[CrossRef](#)]
4. Farah, S.; Anderson, D.G.; Langer, R. Physical and mechanical properties of PLA, and their functions in widespread applications—A comprehensive review. *Adv. Drug Deliv. Rev.* **2016**, *107*, 367–392. [[CrossRef](#)] [[PubMed](#)]
5. Armentano, I.; Bitinis, N.; Fortunati, E.; Mattioli, S.; Rescignano, N.; Verdejo, R.; Lopez-Manchado, M.A.; Kenny, J.M. Multifunctional nanostructured PLA materials for packaging and tissue engineering. *Prog. Polym. Sci.* **2013**, *38*, 1720–1747. [[CrossRef](#)]
6. Nagarajan, V.; Mohanty, A.K.; Misra, M. Perspective on Poly(lactic acid) (PLA) based sustainable materials for durable applications: Focus on toughness and heat resistance. *ACS Sustain. Chem. Eng.* **2016**, *4*, 2899–2916. [[CrossRef](#)]
7. Michalski, A.; Brzezinski, M.; Lapienis, G.; Biela, T. Star-shaped and branched polylactides: Synthesis, characterization, and properties. *Prog. Polym. Sci.* **2019**, *89*, 159–212. [[CrossRef](#)]
8. Lim, L.T.; Auras, R.; Rubino, M. Processing technologies for poly(lactic acid). *Prog. Polym. Sci.* **2008**, *33*, 820–852. [[CrossRef](#)]
9. Harris, A.M.; Lee, E.C. Improving mechanical performance of injection molded PLA by controlling crystallinity. *J. Appl. Polym. Sci.* **2008**, *107*, 2246–2255. [[CrossRef](#)]
10. Tsuji, H. Poly(lactic acid) stereocomplexes: A decade of progress. *Adv. Drug Deliv. Rev.* **2016**, *107*, 97–135. [[CrossRef](#)]
11. Tsuji, H. Poly(lactide) stereocomplexes: Formation, structure, properties, degradation, and applications. *Macromol. Biosci.* **2005**, *5*, 569–597. [[CrossRef](#)] [[PubMed](#)]
12. Ikada, Y.; Jamshidi, K.; Tsuji, H.; Hyon, S.H. Stereocomplex formation between enantiomeric poly(lactides). *Macromolecules* **1987**, *20*, 904–906. [[CrossRef](#)]
13. Fukushima, K.; Kimura, Y. Stereocomplexed polylactides (Neo-PLA) as high-performance bio-based polymers: Their formation, properties, and application. *Polym. Int.* **2006**, *55*, 626–642. [[CrossRef](#)]
14. Tsuji, H.; Ikada, Y. Stereocomplex formation between enantiomeric poly(lactic acid)s. XI. Mechanical properties and morphology of solution-cast films. *Polymer* **1999**, *40*, 6699–6708. [[CrossRef](#)]
15. Pan, G.; Xu, H.; Ma, B.; Wizi, J.; Yang, Y. Polylactide fibers with enhanced hydrolytic and thermal stability via complete stereocomplexation of poly(L-lactide) with high molecular weight of 600000 and lower-molecular-weight poly(D-lactide). *J. Mater. Sci.* **2018**, *53*, 5490–5500. [[CrossRef](#)]
16. Gupta, A.; Katiyar, V. Cellulose functionalized high molecular weight stereocomplex polylactic acid biocomposite films with improved gas barrier, thermomechanical properties. *ACS Sustain. Chem. Eng.* **2017**, *5*, 6835–6844. [[CrossRef](#)]
17. Oyama, H.T.; Abe, S. Stereocomplex poly(lactic acid) alloys with superb heat resistance and toughness. *ACS Sustain. Chem. Eng.* **2015**, *3*, 3245–3252. [[CrossRef](#)]
18. Liu, Z.W.; Luo, Y.L.; Bai, H.W.; Zhang, Q.; Fu, Q. Remarkably enhanced impact toughness and heat resistance of poly(L-lactide)/thermoplastic polyurethane blends by constructing stereocomplex crystallites in the matrix. *ACS Sustain. Chem. Eng.* **2016**, *4*, 111–120. [[CrossRef](#)]
19. Brizzolara, D.; Cantow, H.J.; Diederichs, K.; Keller, E.; Domb, A.J. Mechanism of the stereocomplex formation between enantiomeric poly(lactide)s. *Macromolecules* **1996**, *29*, 191–197. [[CrossRef](#)]
20. Tsuji, H.; Ikada, Y. Stereocomplex formation between enantiomeric poly(lactic acid)s. 9. stereocomplexation from the melt. *Macromolecules* **1993**, *26*, 6918–6926. [[CrossRef](#)]
21. Pan, P.J.; Han, L.L.; Bao, J.N.; Xie, Q.; Shan, G.R.; Bao, Y.Z. Competitive stereocomplexation, homocrystallization, and polymorphic crystalline transition in poly(L-lactide)/poly(D-lactide) racemic blends: Molecular weight effects. *J. Phys. Chem. B* **2015**, *119*, 6462–6470. [[CrossRef](#)] [[PubMed](#)]
22. Li, Y.; Han, C.; Bian, Y.; Dong, Q.; Zhao, H.; Zhang, X.; Xu, M.; Dong, L. Miscibility, thermal properties and polymorphism of stereocomplexation of high-molecular-weight polylactide/poly(D, L-lactide) blends. *Thermochim. Acta* **2014**, *580*, 53–62. [[CrossRef](#)]
23. Kakuta, M.; Hirata, M.; Kimura, Y. Stereoblock polylactides as high-performance bio-based polymers. *Polym. Rev.* **2009**, *49*, 107–140. [[CrossRef](#)]
24. Bao, R.Y.; Yang, W.; Jiang, W.R.; Liu, Z.Y.; Xie, B.H.; Yang, M.B.; Fu, Q. Stereocomplex formation of high-molecular-weight polylactide: A low temperature approach. *Polymer* **2012**, *53*, 5449–5454. [[CrossRef](#)]
25. Tsuji, H.; Tashiro, K.; Bouapao, L.; Hanesaka, M. Synchronous and separate homo-crystallization of enantiomeric poly(l-lactide)/poly(d-lactide) blends. *Polymer* **2012**, *53*, 747–754. [[CrossRef](#)]
26. Tsuji, H.; Iguchi, K.; Arakawa, Y. Stereocomplex- and homo-crystallization behavior, structure, morphology, and thermal properties of crystalline and amorphous stereo diblock copolymers, enantiomeric poly(l-lactide)-b-poly(dl-lactide) and Poly(d-lactide)-b-Poly(dl-lactide). *Polymer* **2021**, *213*, 123226. [[CrossRef](#)]
27. Bai, H.W.; Liu, H.L.; Bai, D.Y.; Zhang, Q.; Wang, K.; Deng, H.; Chen, F.; Fu, Q. Enhancing the melt stability of polylactide stereocomplexes using a solid-state cross-linking strategy during a melt-blending process. *Polym. Chem.* **2014**, *5*, 5985–5993. [[CrossRef](#)]

28. Bai, H.W.; Deng, S.H.; Bai, D.Y.; Zhang, Q.; Fu, Q. Recent advances in processing of stereocomplex-type polylactide. *Macromol. Rapid Commun.* **2017**, *38*, 1700454. [[CrossRef](#)]
29. Hirata, M.; Kimura, Y. Thermo mechanical properties of stereoblock poly (lactic acid) s with different PLLA/PDLA block compositions. *Polymer* **2008**, *49*, 2656–2661. [[CrossRef](#)]
30. Han, L.L.; Xie, Q.; Bao, J.; Shan, G.; Bao, Y.; Pan, P.J. Click chemistry synthesis, stereocomplex formation, and enhanced thermal properties of well-defined poly (l-lactic acid)-b-poly (d-lactic acid) stereo diblock copolymers. *Polym. Chem.* **2017**, *8*, 1006–1016. [[CrossRef](#)]
31. Zhou, D.; Shao, J.; Sun, J.; Bian, X.; Xiang, S.; Li, G.; Chen, X. Effect of the different architectures and molecular weights on stereocomplex in enantiomeric polylactides-b-MPEG block copolymers. *Polymer* **2017**, *123*, 49–54. [[CrossRef](#)]
32. Shao, J.; Sun, J.; Bian, X.; Cui, Y.; Li, G.; Chen, X. Investigation of poly(lactide) stereocomplexes: 3-armed poly (L-lactide) blended with linear and 3-armed enantiomers. *J. Phys. Chem. B* **2012**, *116*, 9983–9991. [[CrossRef](#)] [[PubMed](#)]
33. Sakamoto, Y.; Tsuji, H. Crystallization behavior and physical properties of linear 2-arm and branched 4-arm poly (l-lactide)s: Effects of branching. *Polymer* **2013**, *54*, 2422–2434. [[CrossRef](#)]
34. Han, L.L.; Shan, G.R.; Bao, Y.Z.; Pan, P.J. Exclusive stereocomplex crystallization of Linear and multiarm star-shaped high-molecular-weight stereo diblock poly(lactic acid)s. *J. Phys. Chem. B* **2015**, *119*, 14270–14279. [[CrossRef](#)] [[PubMed](#)]
35. Chang, Y.; Chen, Z.; Pan, G.; Yang, Y. Enhancing the recrystallization ability of bio-based polylactide stereocomplex by in situ construction of multi-block branched conformation. *J. Mater. Sci.* **2019**, *54*, 12145–12158. [[CrossRef](#)]
36. Bai, H.W.; Bai, D.Y.; Xiu, H.; Liu, H.L.; Zhang, Q.; Wang, K.; Deng, H.; Chen, F.; Fu, Q.; Chiu, F.C. Towards high-performance poly (L-lactide)/elastomer blends with tunable interfacial adhesion and matrix crystallization via constructing stereocomplex crystallites at the interface. *RSC Adv.* **2014**, *4*, 49374–49385. [[CrossRef](#)]
37. Ma, P.; Jiang, L.; Xu, P.; Dong, W.; Chen, M.; Lemstra, P.J. Rapid stereocomplexation between enantiomeric comb-shaped cellulose-g-poly (L-lactide) nanohybrids and poly (D-lactide) from the melt. *Biomacromolecules* **2015**, *16*, 3723–3729. [[CrossRef](#)]
38. Deng, S.H.; Bai, H.W.; Liu, Z.W.; Zhang, Q.; Fu, Q. Toward supertough and heat-resistant stereocomplex-type polylactide/elastomer blends with impressive melt stability via in situ formation of graft copolymer during one-pot reactive melt blending. *Macromolecules* **2019**, *52*, 1718–1730. [[CrossRef](#)]
39. Cheerarat, O.; Baimark, Y. Thermal and mechanical properties of biodegradable star-shaped/linear polylactide stereocomplexes. *J. Chem.* **2015**, *2015*, 206123. [[CrossRef](#)]
40. Biela, T. Stereocomplexes of star-shaped poly (R)-lactide s and poly (S)-lactide s bearing various number of arms. Synthesis and thermal properties. *Polimery* **2007**, *52*, 106–116. [[CrossRef](#)]
41. Bao, J.N.; Han, L.L.; Shan, G.; Bao, Y.; Pan, P.J. Preferential stereocomplex crystallization in enantiomeric blends of cellulose acetate-g-poly (lactic acid) s with comblike topology. *J. Phys. Chem. B* **2015**, *119*, 12689–12698. [[CrossRef](#)] [[PubMed](#)]
42. Cui, L.; Zhang, R.; Wang, Y. Effect of plasticizer poly (ethylene glycol) on the crystallization properties of stereocomplex-type poly (lactide acid). *Wuhan Univ. J. Nat. Sci.* **2017**, *22*, 420–428. [[CrossRef](#)]
43. Cui, L.; Wang, Y.; Zhang, R.; Liu, Y. Design high heat-resistant stereocomplex poly (lactide acid) by cross-linking and plasticizing. *Adv. Polym. Technol.* **2018**, *37*, 2429–2435. [[CrossRef](#)]
44. Anakabe, J.; Zaldua Huici, A.M.; Eceiza, A.; Arbelaz, A.; Averous, L. Combined effect of nucleating agent and plasticizer on the crystallization behaviour of polylactide. *Polym. Bull.* **2017**, *74*, 4857–4886. [[CrossRef](#)]
45. Wu, B.G.; Yang, W.J.; Niu, D.Y.; Dong, W.F.; Chen, M.Q.; Liu, T.X.; Du, M.L.; Ma, P.M. Stereocomplexed poly(lactide) composites toward engineering plastics with superior toughness, heat resistance and anti-hydrolysis. *Chin. J. Polym. Sci.* **2020**, *38*, 1107–1116. [[CrossRef](#)]
46. Li, Y.; Han, C.; Zhang, X.; Dong, Q.; Dong, L. Effects of molten poly (D, L-lactide) on nonisothermal crystallization in stereocomplex of poly (L-lactide) with poly (D-lactide). *Thermochim. Acta* **2013**, *573*, 193–199. [[CrossRef](#)]
47. Xie, Q.; Han, L.L.; Shan, G.; Bao, Y.; Pan, P.J. Promoted stereocomplex formation and two-step crystallization kinetics of poly (L-lactic acid)/poly (D-lactic acid) blends induced by nucleator. *Polym. Cryst.* **2019**, *2*, e10057. [[CrossRef](#)]
48. Xie, Q.; Han, L.L.; Shan, G.; Bao, Y.; Pan, P.J. Polymorphic Crystalline Structure and Crystal Morphology of Enantiomeric Poly (lactic acid) Blends Tailored by a Self-Assemblable Aryl Amide Nucleator. *ACS Sustain. Chem. Eng.* **2016**, *4*, 2680–2688. [[CrossRef](#)]
49. Chen, Y.; Hua, W.Q.; Zhang, Z.C.; Xu, J.Z.; Bian, F.G.; Zhong, G.J.; Xu, L.; Li, Z.M. An efficient, food contact accelerator for stereocomplexation of high-molecular-weight poly (L-lactide)/poly (D-lactide) blend under nonisothermal crystallization. *Polymer* **2019**, *170*, 54–64. [[CrossRef](#)]
50. Cao, Z.Q.; Sun, X.R.; Bao, R.Y.; Yang, W.; Xie, B.H.; Yang, M.B. Role of carbon nanotube grafted poly(l-lactide)-block-poly (d-lactide) in the crystallization of poly (l-lactic acid)/poly (d-lactic acid) blends: Suppressed homocrystallization and enhanced stereocomplex crystallization. *Eur. Polym. J.* **2016**, *83*, 42–52. [[CrossRef](#)]
51. Bao, R.Y.; Yang, W.; Wei, X.F.; Xie, B.H.; Yang, M.B. Enhanced formation of stereocomplex crystallites of high molecular weight poly(L-lactide)/poly(D-lactide) blends from melt by using poly (ethylene glycol). *ACS Sustain. Chem. Eng.* **2014**, *2*, 2301–2309. [[CrossRef](#)]
52. Samuel, C.; Cayuela, J.; Barakat, I.; Mueller, A.J.; Raquez, J.M.; Dubois, P. Stereocomplexation of polylactide enhanced by poly (methyl methacrylate): Improved processability and thermomechanical properties of stereocomplexable polylactide-based materials. *ACS Appl. Mater. Interfaces* **2013**, *5*, 11797–11807. [[CrossRef](#)] [[PubMed](#)]

53. Dong, Q.; Bian, Y.; Li, Y.; Han, C.; Dong, L. Miscibility and crystallization behaviors of stereocomplex-type poly (L- and D-lactide)/poly (methyl methacrylate) blends. *J. Therm. Anal. Calorim.* **2014**, *118*, 359–367. [[CrossRef](#)]
54. Bao, R.Y.; Yang, W.; Liu, Z.Y.; Xie, B.H.; Yang, M.B. Polymorphism of a high-molecular-weight racemic poly(L-lactide)/poly(D-lactide) blend: Effect of melt blending with poly (methyl methacrylate). *RSC Adv.* **2015**, *5*, 19058–19066. [[CrossRef](#)]
55. Pan, P.J.; Bao, J.N.; Han, L.L.; Xie, Q.; Shan, G.; Bao, Y. Stereocomplexation of high-molecular-weight enantiomeric poly (lactic acid) s enhanced by miscible polymer blending with hydrogen bond interactions. *Polymer* **2016**, *98*, 80–87. [[CrossRef](#)]
56. Bao, J.N.; Xue, X.; Li, K.; Chang, X.; Xie, Q.; Yu, C.; Pan, P.J. Competing stereocomplexation and homocrystallization of poly (l-lactic acid)/poly (d-lactic acid) racemic mixture: Effects of miscible blending with other polymers. *J. Phys. Chem. B* **2017**, *121*, 6934–6943. [[CrossRef](#)]
57. Deng, S.H.; Yao, J.; Bai, H.W.; Xiu, H.; Zhang, Q.; Fu, Q. A generalizable strategy toward highly tough and heat-resistant stereocomplex-type polylactide/elastomer blends with substantially enhanced melt processability. *Polymer* **2021**, *224*, 123736. [[CrossRef](#)]
58. Xu, H.; Fang, H.; Bai, J.; Zhang, Y.; Wang, Z. Preparation and characterization of high-melt-strength polylactide with long-chain branched structure through γ -radiation-induced chemical reactions. *Ind. Eng. Chem. Res.* **2014**, *53*, 1150–1159. [[CrossRef](#)]
59. Liu, J.; Zhang, S.; Zhang, L.; Bai, Y. Crystallization behavior of long-chain branching polylactide. *Ind. Eng. Chem. Res.* **2012**, *51*, 13670–13679. [[CrossRef](#)]
60. Bousmina, M.; Ait-Kadi, A.; Faisant, J.B. Determination of shear rate and viscosity from batch mixer data. *J. Rheol.* **1999**, *43*, 415–433. [[CrossRef](#)]
61. Ma, P.; Shen, T.; Xu, P.; Dong, W.; Lemstra, P.J.; Chen, M. Superior performance of fully biobased poly (lactide) via stereocomplexation-induced phase separation: Structure versus property. *ACS Sustainable. Chem. Eng.* **2015**, *3*, 1470–1478. [[CrossRef](#)]
62. Bao, R.Y.; Yang, W.; Jiang, W.R.; Liu, Z.Y.; Xie, B.H.; Yang, M.B. Polymorphism of racemic poly (L-lactide)/poly (D-lactide) blend: Effect of melt and cold crystallization. *J. Phys. Chem. B* **2013**, *117*, 3667–3674. [[CrossRef](#)] [[PubMed](#)]
63. Yang, C.F.; Huang, Y.F.; Ruan, J.; Su, A.C. Extensive development of precursory helical pairs prior to formation of stereocomplex crystals in racemic polylactide melt mixture. *Macromolecules* **2012**, *45*, 872–878. [[CrossRef](#)]
64. Feng, L.; Bian, X.; Li, G.; Chen, X. Thermal Properties and Structural Evolution of Poly (l-lactide)/Poly (d-lactide) Blends. *Macromolecules* **2021**, *54*, 10163–10176. [[CrossRef](#)]